Collateral Sensitivity Interactions between Antibiotics Depend on Local Abiotic Conditions

Richard C. Allen,ᵃ* Katia R. Pfrunder-Cardozo,ᵃ Alex R. Hallᵃ

ᵃDepartment of Environmental Systems Science, ETH Zürich, Zürich, Switzerland

ABSTRACT Mutations conferring resistance to one antibiotic can increase (cross-resistance) or decrease (collateral sensitivity) resistance to others. Antibiotic combinations displaying collateral sensitivity could be used in treatments that slow resistance evolution. However, lab-to-clinic translation requires understanding whether collateral effects are robust across different environmental conditions. Here, we isolated and characterized resistant mutants of *Escherichia coli* using five antibiotics, before measuring collateral effects on resistance to other paired antibiotics. During both isolation and phenotyping, we varied conditions in ways relevant in nature (pH, temperature, and bile). This revealed that local abiotic conditions modified expression of resistance against both the antibiotic used during isolation and other antibiotics. Consequently, local conditions influenced collateral sensitivity in two ways: by favoring different sets of mutants (with different collateral sensitivities) and by modifying expression of collateral effects for individual mutants. These results place collateral sensitivity in the context of environmental variation, with important implications for translation to real-world applications.

IMPORTANCE When bacteria become resistant to an antibiotic, the genetic changes involved sometimes increase (cross-resistance) or decrease (collateral sensitivity) their resistance to other antibiotics. Antibiotic combinations showing repeatable collateral sensitivity could be used in treatment to slow resistance evolution. However, collateral sensitivity interactions may depend on the local environmental conditions that bacteria experience, potentially reducing repeatability and clinical application. Here, we show that variation in local conditions (pH, temperature, and bile salts) can influence collateral sensitivity in two ways: by favoring different sets of mutants during bacterial resistance evolution (with different collateral sensitivities to other antibiotics) and by modifying expression of collateral effects for individual mutants. This suggests that translation from the lab to the clinic of new approaches exploiting collateral sensitivity will be influenced by local abiotic conditions.

KEYWORDS antibiotic resistance, collateral sensitivity

As a result of antibiotic use, resistance is increasing in bacteria (1), necessitating efforts to identify new antibiotic types (2). However, the time, money, and risks involved in getting new therapeutics to the clinic (3) and the targeting of many essential bacterial pathways by existing antibiotics mean that the rate of development for new antibiotics is outstripped by rates of resistance development (3). To tackle the threat of antibiotic resistance, we must investigate strategies to slow the spread of resistance to existing treatments and to any new treatments in development (4). One strategy that shows promise in slowing the evolution of resistance is to exploit collateral sensitivity interactions (5–8). These have been observed for specific combinations of antibiotics where mutations conferring resistance to one antibiotic sensitize bacteria to a second antibiotic (5–8), thereby increasing the effectiveness of the second antibiotic and reducing the potential for resistance evolution to it (6, 9). For collateral sensitivity interactions to be exploited

Address correspondence to Richard C. Allen, richardcharles.allen@uzh.ch.

*Present address: Richard C. Allen, Department of Quantitative Bioscience, University of Zürich, Zürich, Switzerland.

therapeutically, it is important that their emergence across different populations of bacteria, such as those in different patients or in different communities, be repeatable. That is, unless collateral sensitivity interactions are predictable, exploiting them in new treatment strategies will be very challenging (10–13).

Recent work revealed important genetic factors influencing the predictability of collateral sensitivity, but the importance of local abiotic conditions is still unclear. For example, high-throughput *in vitro* studies showed that different replicate populations exposed to the same antibiotic sometimes acquire collateral sensitivity to another antibiotic and sometimes do not (10, 11). This can be explained by different mutations, which vary in their phenotypic effects on resistance, spreading in different replicate populations (11, 12, 14, 15). However, we know from past work that phenotypic effects of antibiotic resistance mechanisms also vary strongly depending on local environmental conditions (16–19). For example, bile can upregulate efflux pumps (20), zinc can reduce the activity of aminoglycoside-degrading enzymes (21), and high temperature can modulate the effects of rifampicin resistance mutations on growth in the absence of antibiotics (22). This raises the possibility that local environmental conditions could influence the emergence of collateral sensitivity by affecting which of the possible pathways to resistance are most strongly selected, both in the absence of antibiotics and during antibiotic exposure. Furthermore, the abiotic environment could affect the expression of collateral effects, by modifying the phenotypic effects of resistance alleles when bacteria are exposed to a second antibiotic. To date, research on collateral sensitivity interactions has focused on testing many combinations of antibiotics (5, 6, 9, 14), multiple strains (10), or many replicate populations for individual antibiotic combinations (11). Therefore, the role of local abiotic conditions in the emergence and expression of collateral sensitivity interactions remains unclear. Answering this question would improve our understanding of the robustness of collateral sensitivity across different populations and environments. This would in turn boost our ability to predict pathogen responses to treatment regimens that exploit collateral sensitivity interactions.

To address these gaps in our knowledge, we tested for collateral effects (cross-resistance or collateral sensitivity) between five pairs of antibiotics, each in four different experimental environments. Each antibiotic pair consisted of a selection antibiotic (which we used in mutant isolation) and a paired antibiotic (which we used to test for collateral effects). We chose pairs of antibiotics indicated by past work to at least sometimes display collateral sensitivity interactions (5, 6). The four experimental environments were (i) basal, nutrient-rich broth (lysogeny broth [LB] at 37°C and buffered at pH 7.0), plus three types of abiotic environmental variation which we expect to be relevant to pathogens *in vivo*; (ii) reduced pH (pH 6.5), as found in certain body compartments, including abscesses and parts of the gastrointestinal (GI) tract (23, 24); (iii) increased temperature (42°C), as found in companion and livestock animals with higher core temperatures than humans (25); and (iv) the presence of bile salts (0.5 g/L bile salts), which bacteria must contend with in the GI tract (26).

In each of four sets of abiotic conditions, we grew multiple independent populations of *Escherichia coli* K-12 MG1655 in the absence of antibiotics, before screening for antibiotic-resistant mutants, on agar with the selection antibiotic (shown schematically in Fig. S1 in the supplemental material). From these resistant mutants, we randomly chose single colonies (from independent populations) to isolate and sequence. For each isolate, we then measured resistance as the 90% inhibitory concentration (IC_{90}) for the relevant selection antibiotic and paired antibiotic, again across all four sets of abiotic conditions (Fig. S1). Unlike past work, this manipulation of the experimental environment, during both isolation and phenotyping, in a fully factorial design allowed us to quantify the effects of local abiotic conditions on the emergence (which mutations are selected in which treatments?) and expression (in which abiotic environments do we see collateral effects from particular mutants?) of collateral sensitivity for multiple candidate antibiotic pairs. Our aim was to quantify the effect of environmental conditions on collateral sensitivity interactions for a range of different mutants, rather than
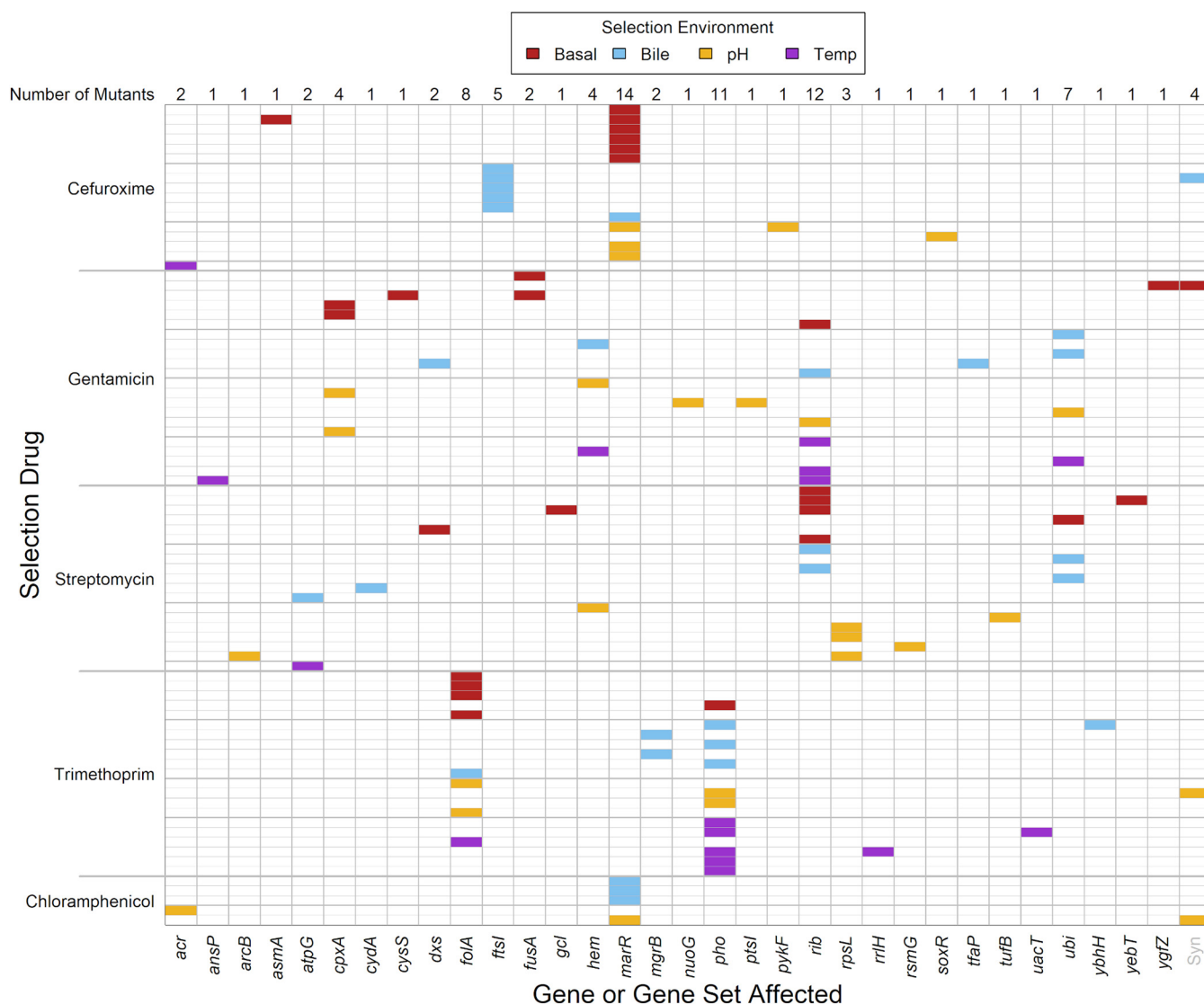
FIG 1 Genes affected by mutations, in mutants selected for resistance to different antibiotics in different selection environments. Each row of cells represents one mutant; rows are grouped by which antibiotic they were selected against (selection drug; labeled at left) and colored by the abiotic conditions during selection (selection environment; legend at top with the following abbreviations: basal, basal conditions of pH 7.0 and 37°C; bile, with added bile salts at 0.5 g/L; pH, with reduced pH of 6.5; temp, increased temperature of 42°C). Each column of cells represents one gene or gene set that was affected by mutations in our isolated mutants (ordered alphabetically). Each gene set comprises multiple genes involved in the same pathway (see Materials and Methods); these were *acr*, *hem*, *pho*, *rib*, and *ubi*. At the top, the total number of mutants with mutations affecting each gene is shown. Sixteen of the 84 mutants contained multiple mutations affecting multiple genes, all of which are shown. The rightmost column (Syn) shows synonymous mutations, found in four mutants (all four mutants also had other, nonsynonymous mutations). For more information, see Table S1.

to focus on individual mutations. Nevertheless, for some of the mutations we identified, existing information about their physiological effects provides mechanistic insight into the origins of observed collateral effects, and we place our findings in this context where relevant.

RESULTS

Different resistance mutations isolated depending on local abiotic conditions. We used whole-genome sequencing to identify genetic changes relative to the ancestral strain for 84 resistant mutants (Fig. 1; Table S1), each isolated after exposure to one of five antibiotics (selection antibiotic, defined as the antibiotic present in the agar plate used to select resistant mutants from ancestral cells) in four different abiotic environments (selection environment, defined as the local abiotic conditions during overnight growth prior to plating and in the agar plate). We found that mutants selected

with the same selection antibiotic tended to have mutations affecting the same genes more often than mutants selected with different selection antibiotics (permutational multivariate analysis of variance [PERMANOVA]: $F_{3,72}$ = 7.21; P < 0.001). Similarly, mutants selected in the same selection environment tended to have mutations affecting the same genes more often than mutants selected in different selection environments (PERMANOVA: $F_{3,75}$ = 2.44; P < 0.001). Looking at each selection antibiotic separately, there was an effect of selection environment for cefuroxime ($F_{3,13}$ = 7.50; corrected P < 0.01) and streptomycin ($F_{3,15}$ = 2.19; corrected P < 0.05) but not trimethoprim and gentamicin (corrected P > 0.05). For streptomycin, the major differences were between the mutations selected in the low-pH environment and those in other selection environments. For cefuroxime, we found mutations in the penicillin-binding protein gene *ftsI*, but only in the presence of bile (Fig. 1). For chloramphenicol, we obtained genotypic information for only five mutants; these are shown in Fig. 1 and Fig. S2 but not included in the analyses here or below because of the much smaller sample size. In summary, the types of resistance mechanisms that were selected during our mutant screen depended on the local abiotic conditions.

Collateral sensitivity and cross-resistance vary depending on resistance mechanism. We tested whether different resistant mutants showed variable susceptibility to paired antibiotics previously implicated in collateral sensitivity. For the selection antibiotics cefuroxime, gentamicin, streptomycin, and trimethoprim, the paired antibiotics were gentamicin (6), cefuroxime (6), tetracycline (5), and nitrofurantoin (5), respectively. The average fold change in IC_{90} of paired antibiotics was low (mean ± standard deviation of log_2-transformed relative IC_{90}, 0.01 ± 0.71) (Fig. 2 and Fig. S3) compared to changes in resistance to the selection antibiotics (1.99 ± 1.13) (Fig. 2 and Fig. S3; discussed further below) and encompassed both positive (cross-resistance) and negative (collateral sensitivity) changes in resistance (Fig. 2). For individual pairs of antibiotics, average collateral effects varied depending on which gene was mutated for the sets of mutants selected against gentamicin and then tested against cefuroxime (main effect of genotype on cefuroxime IC_{90}: $F_{4,46}$ = 6.73; corrected P < 0.01), mutants selected against streptomycin and tested against tetracycline ($F_{5,139}$ = 3.93; corrected P < 0.01), and mutants selected against trimethoprim and tested against nitrofurantoin (χ^2_2 = 10.8; corrected P < 0.01) but not for mutants selected against cefuroxime and tested against gentamicin ($F_{4,19}$ = 0.189, corrected P > 0.5). We found several genes that were consistently associated with collateral sensitivity to paired antibiotics (shown by negative values of log_2-transformed relative IC_{90}), such as *ubi* mutants, which were on average collaterally sensitive to cefuroxime (effect of *ubi* mutation on log_2-transformed relative IC_{90}: $\beta = -0.98$: t_{38} = 3.51; P < 0.001) (Fig. 2b), and *atpG* mutants, which were on average collaterally sensitive to tetracycline ($\beta = -0.452$; t_{148} = 3.27; P < 0.01) (Fig. 2c). Mutations in *ubi* genes and in *atpG* affect ubiquinone synthesis and the ATP synthase, respectively, disrupting the proton motive force (PMF), which in turn leads to a reduced membrane potential and hence reduced influx of aminoglycosides (27). Despite the benefit of aminoglycoside resistance, PMF-driven efflux pumps such as acrAB are less active in mutants with disrupted PMF (5), increasing susceptibility to other antibiotics.

For mutants selected against trimethoprim, the variable collateral effects observed for different mutants/genotypes translated to differences in average resistance to nitrofurantoin depending on which environment they were selected in (effect of selection environment on IC_{90} to nitrofurantoin: χ^2_3 = 20.6; corrected P < 0.01). Mutants selected at high temperature ($\beta = -0.26$; t_{58} = 4.19; P < 0.05) had significant collateral sensitivity. Mutations in *phoPQ*, which were associated with relatively high sensitivity to nitrofurantoin (Fig. 2d), were more common at high temperature than in the other selection environments (Fig. 1). In summary, mutants selected for resistance to one antibiotic often had altered average resistance to other antibiotics (as expected, as these antibiotics were chosen based on past evidence of such effects). However, these collateral effects varied among different pathways to resistance (mutated genes), which
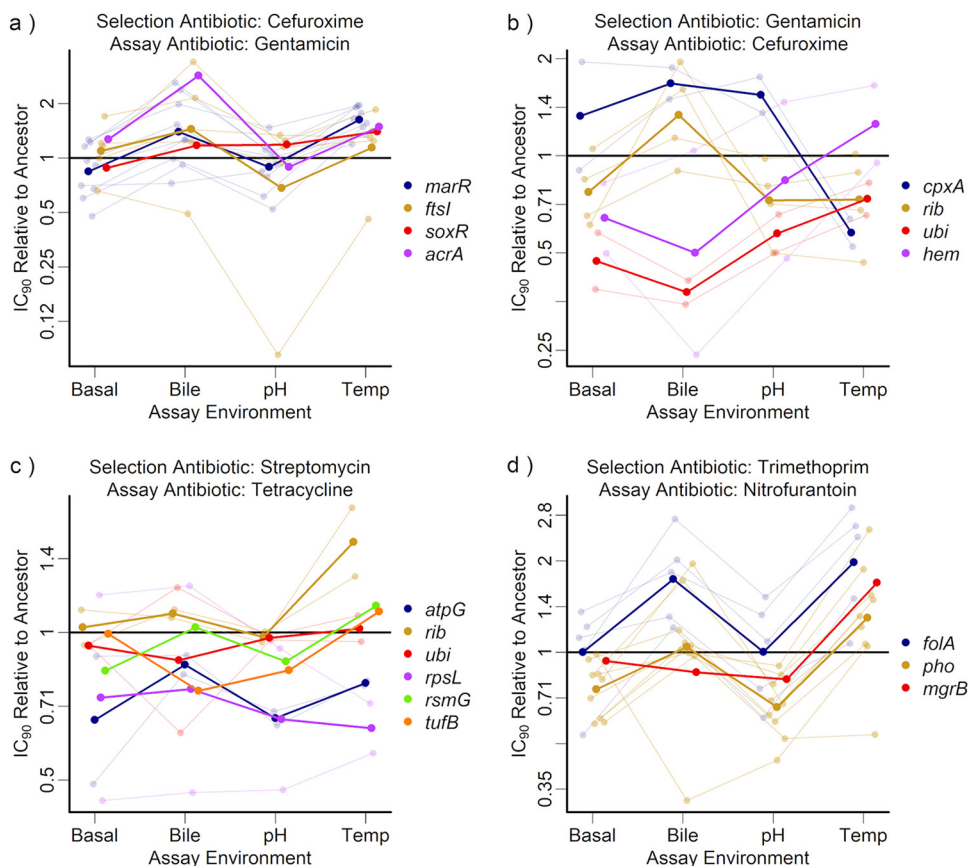
FIG 2 Collateral changes in resistance to a paired antibiotic for resistant mutants selected with each selection antibiotic, tested across different abiotic conditions (x axis, assay environments). Each panel shows mutants selected for resistance to a selection antibiotic and then tested for resistance to a paired antibiotic (labeled at the top of the panel). The IC_{90} for each mutant of the paired drug is shown relative to the ancestor in the same environment (scores for the ancestor are given in Fig. S3): mutants with points of >1 are more resistant and those with points of <1 are more sensitive than the ancestor. Mutants are grouped and colored according to the gene or gene set that was mutated; the thick lines show mean IC_{90} across all mutants with the same gene/gene set mutated. Where there were multiple mutants with the same gene/gene set mutated, thin lines show IC_{90}s for the individual mutants. The y axis is log transformed, and the scale varies between panels.

translated in some cases to variation of average collateral effects depending on the abiotic conditions during selection for resistance to the first antibiotic (selection environment).

Collateral effects depend on the assay environment. Expression of average collateral effects to paired antibiotics also varied depending on the abiotic conditions during exposure to these antibiotics. For mutants selected against cefuroxime and trimethoprim, there was a significant effect of assay environment on average resistance to the paired antibiotics, relative to the ancestor under the same conditions (effect of assay environment on resistance to paired antibiotic for selection-paired antibiotic: cefuroxime-gentamicin, $\chi^2_3 = 53.0$, corrected $P < 0.001$; trimethoprim-nitrofurantoin, $\chi^2_3 = 89.1$, corrected $P < 0.001$) (Fig. 2). Note that this variation of susceptibility relative to the ancestral strain was not explained by variable susceptibility of the ancestral strain across assay environments (Fig. S3). Qualitatively similar results emerge (see the legend to Fig. S3) if we use the absolute IC_{90} (not relative to the ancestor).

Changing the local abiotic conditions did not affect all mutants the same way: the mutated gene and assay environment interacted to determine resistance to cefuroxime in mutants selected against gentamicin (genotype-by-assay environment interaction effect on cefuroxime resistance: $\chi^2_9 = 38.3$; corrected $P < 0.001$). For some mutants, this variation led to a switch between cross-resistance and collateral sensitivity, such as *cpxA* mutants (Fig. 2b), which were resistant to cefuroxime in the bile ($\beta =$

0.74; t_{130} = 2.48; $P < 0.05$) and pH (β = 0.63; t_{130} = 2.09; $P < 0.05$) environments but were susceptible to cefuroxime at high temperature (β = −0.79; t_{130} = 2.64; $P < 0.01$). *cpxA* is part of a two-component regulator which responds to misfolded proteins in the periplasm, activating the Cpx response, which has been shown to confer resistance to aminoglycosides (28). Mutations in the periplasmic domain of *cpxA* (as in our mutants) have the Cpx pathway locked into an activated state (29), with Cpx phenotypes being more pronounced at high temperature (30, 31). Other work has shown that, due to its influence on cell wall homeostasis, the Cpx response can influence resistance to β-lactams like cefuroxime but that it must be at an intermediate level for maximal resistance (32). At temperatures of 37°C, our mutants likely upregulate the Cpx response into the optimum zone, leading to β-lactam resistance. However, at 42°C, the mutant's Cpx response is likely further upregulated (30, 31), meaning that peptidoglycan homeostasis is no longer maintained, resulting in β-lactam sensitivity (32). This shows that collateral effects for individual resistant strains can change qualitatively across different abiotic environments.

Environment-dependent selection for particular genotypes is revealed by analyzing growth at the selecting antibiotic concentration but not resistance as IC$_{90}$. Having found that local abiotic conditions influenced collateral sensitivity by changing both the expression of resistance phenotypes for individual mutants and which mutants we isolated upon antibiotic exposure, we sought to explain why different mutants were isolated in different selection environments. The first possible explanation we tested was that the identity of the mutations conferring most effective resistance against each selection antibiotic (and therefore most likely to form a colony and be detected in our mutant screen) may depend on local abiotic conditions (Fig. S4). We found no statistical support for such an effect when we measured resistance (IC_{90}) of each mutant to its corresponding selection antibiotic in all four abiotic conditions: assay environment did not significantly alter the observed variation of IC_{90} among genotypes (genotype-by-assay-environment interaction: corrected $P > 0.05$ for all antibiotics). Furthermore, we found no evidence that average IC_{90} was higher for mutants tested in sympatric environments (selection environment = assay environment) than in allopatric environments (selection environment $\neq$ assay environment), as would be the case if the mutations we detected conferred bigger increases in resistance in the abiotic conditions they were selected in (33, 34) (difference between sympatric and allopatric combinations: corrected $P > 0.05$ for all selection antibiotics). Thus, variation across assay environments of the relative changes in resistance (measured as IC_{90}) conferred by different resistance mutations did not explain why we isolated different mutants in different conditions (Fig. 1).

We next analyzed an alternative measure of resistance, growth of each mutant at the antibiotic concentration used during selection (GASC). Our rationale here was that the mutations most beneficial during our screen (and most likely to result in formation of viable colonies) are not necessarily the mutations that confer the largest increases in IC_{90}. Therefore, GASC potentially provides additional information about why some types of mutants were associated with particular selection environments. GASC was calculated from the same dose-response curves as the IC_{90} and was positively correlated with IC_{90} across all mutants (correlation: τ = 0.508; $P < 0.0001$) (Fig. S5). For trimethoprim-resistant mutants, GASC was predicted by the interaction between mutated gene and assay environment (gene-by-assay-environment interaction: χ^2_6 = 33.4; corrected $P < 0.001$) (Fig. 3d), and the best-performing individual mutant (thin lines in Fig. 3d) varied among different assay conditions. Trimethoprim-resistant mutants also showed evidence of matching between mutants and their selection environments, in that GASC was higher in sympatric than allopatric combinations (effect of sympatry: β = 0.0818; standard error [SE] = 0.0234; χ^2_1 = 11.8; corrected $P < 0.01$). For cefuroxime-resistant mutants, GASC varied significantly among sets of mutants selected under different abiotic conditions, with bile-selected mutants performing best (effect of selection environment: χ^2_3 = 11.3; corrected $P < 0.05$) (Fig. 3a). Thus, addition of bile biased our screen toward a relatively narrow set of mutants that grew well at the cefuroxime
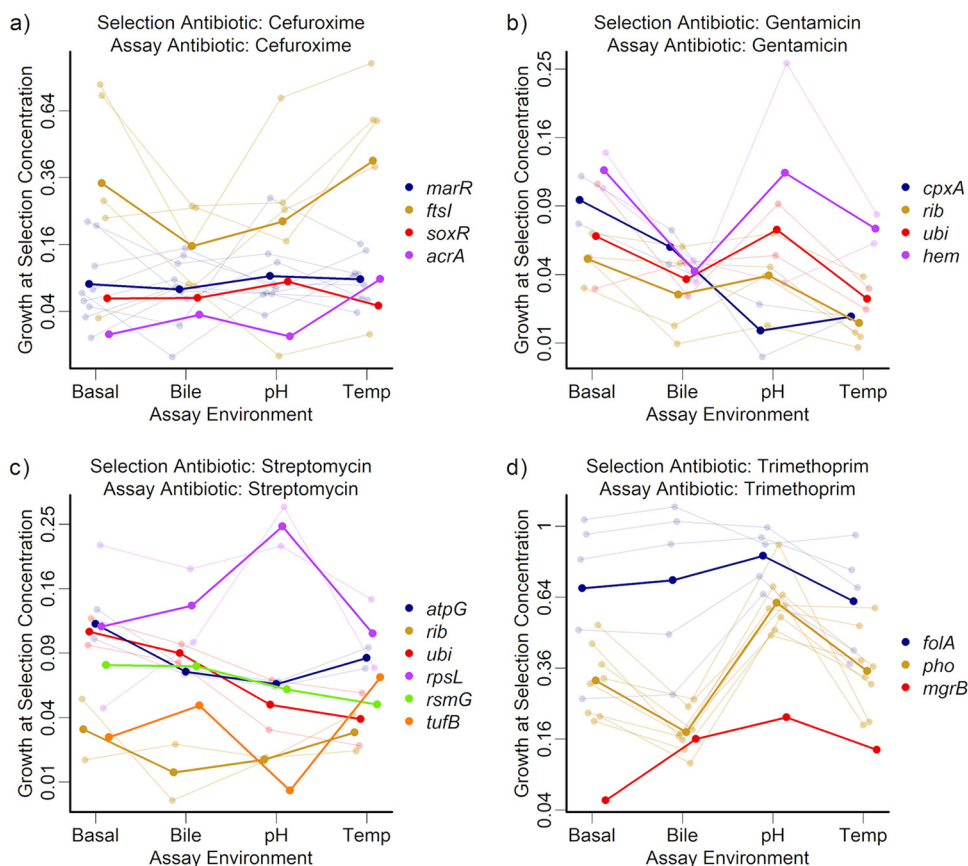
FIG 3 Population growth for resistant mutants selected with each selection drug when grown with that antibiotic at selection concentration (GASC), measured in four different assay environments. Each panel shows mutants selected for resistance to the selection antibiotic shown in the panel title and then assayed for growth at the selection concentration of that drug. Mutants are grouped and colored according to the gene or gene set that was mutated, with the thick lines showing the mean GASC across all strains with the same genotype. Where there were multiple mutants with the same genotype, thin lines show the GASC for the individual mutants. The y axis is square-root transformed and varies between panels.

concentration used during selection (in particular, *ftsI* mutants) (Fig. 1). Consistent with this, we observed resistant colonies in our mutant screen in fewer replicate populations exposed to bile plus cefuroxime than other cefuroxime selection environments (Fig. S6). Despite this, the genotype-by-assay-environment interaction for cefuroxime-resistant mutants was not significant after accounting for multiple testing ($\chi^2_9 = 15.4$; corrected $P > 0.1$). Note that *ftsI* mutants also had relatively high IC_{90} on average (Fig. S4), although this did not translate to significant variation of mean IC_{90} with selection environment, as it did for GASC. Finally, for the relatively small number of chloramphenicol-resistant mutants we tested, we also observed an interaction between mutated gene and assay environment for GASC (Fig. S2c). In summary, analyzing GASC revealed evidence that some selection environments favored particular types of resistance mutations.

Antibiotic-free growth depends on resistance mechanism and local abiotic conditions. Antibiotic resistance is often associated with a fitness cost in terms of impaired growth in the absence of antibiotics, and variation of this cost is a key driver of the long-term persistence of resistance (16, 35). In our mutant selection experiment, bacteria were grown in the absence of antibiotics prior to plating. Because plating was done at antibiotic concentrations that fully inhibited growth of the ancestral strain, we expect resistance mutations that we detected to have arisen predominantly during this first (antibiotic-free) phase (Fig. S1), rather than on the agar plate. Therefore, variable costs of resistance across selection environments could potentially help to explain why we found different sets of mutants in different selection environments. We
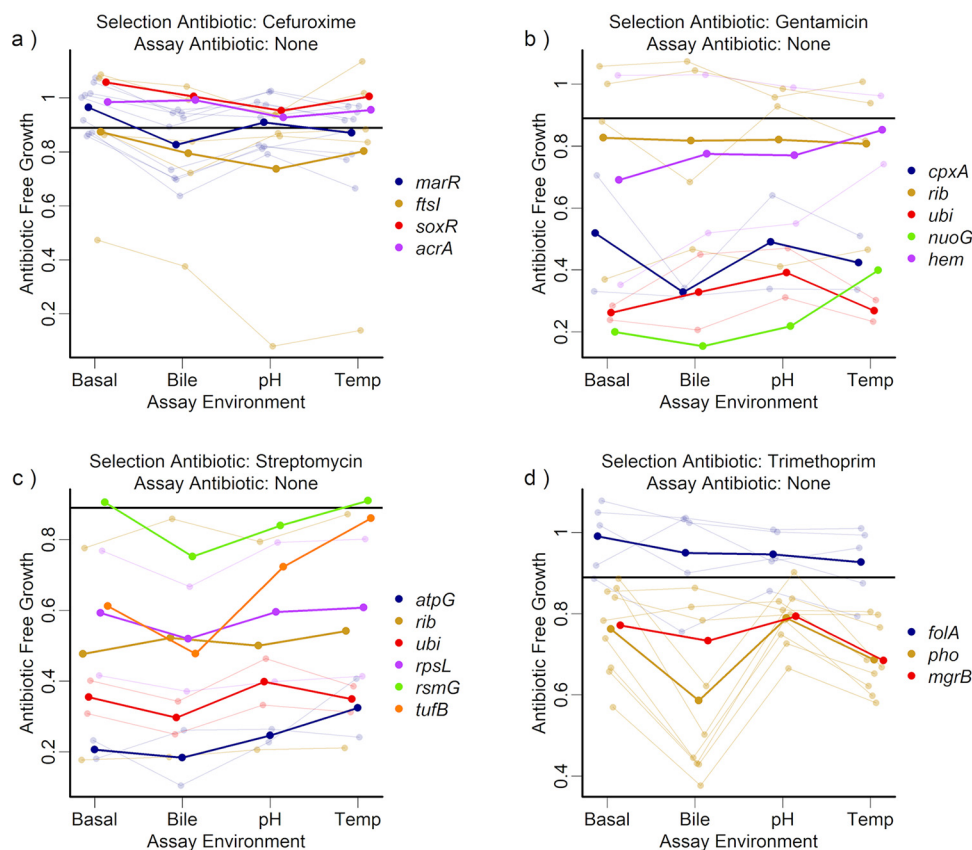
FIG 4 Antibiotic-free growth of resistant mutants selected with each selection antibiotic, measured in four different assay environments. Each panel shows the antibiotic-free growth for mutants selected for resistance to one of four selection drugs, as indicated for each panel. Mutants are grouped and colored according to the gene or gene set that was mutated, with the thick lines showing the mean antibiotic-free growth across all strains with the same genotype. Where there were multiple mutants with the same genotype, thin lines show the antibiotic-free growth for the individual mutants. The black horizontal line in each plot gives the mean antibiotic-free growth of the ancestral strain (across all assay environments). The y axis scale varies between panels.

investigated this by quantifying the growth of each mutant in the absence of antibiotics, using the data set used to calculate the IC$_{90}$s (see Materials and Methods). Relative to the ancestral strain in the absence of antibiotics (mean final optical density $\pm$ standard deviation, 0.898 $\pm$ 0.104), most types of resistant mutants showed evidence of growth costs, with 29 of the 57 mutants showing at least a 20% reduction in mean growth relative to the ancestor in one or more environment. However, this varied depending on the selection antibiotic (cefuroxime, 0.876 $\pm$ 0.194; gentamicin, 0.599 $\pm$ 0.308; streptomycin, 0.488 $\pm$ 0.258; trimethoprim, 0.790 $\pm$ 0.168) (Fig. 4).

For all selection antibiotics, mean antibiotic-free growth varied depending on which gene was mutated (Fig. 4, effect of mutated gene on antibiotic-free growth: cefuroxime-selected mutants, $F_{4,16} = 107$, corrected $P < 0.001$; gentamicin, $F_{5,12} = 23.0$, corrected $P < 0.001$; streptomycin, $F_{6,10} = 15.5$, corrected $P < 0.001$; trimethoprim, $F_{3,18} = 358$, $P < 0.001$). For example, streptomycin-resistant mutants with mutations in *atpG* grew relatively poorly (Fig. 4c) (difference from ancestor: $\beta = -0.66$, $t_{10} = 5.67$, $P < 0.001$), as did trimethoprim-resistant mutants with *phoPQ* mutations (Fig. 4d) (difference from ancestor: $\beta = -0.20$, $t_{15} = 6.84$, $P < 0.001$). For all selection antibiotics, variation of antibiotic-free growth among different genotypes depended on the local abiotic conditions (genotype-by-assay-environment interaction: cefuroxime, $\chi^2_9 = 23.8$, corrected $P < 0.05$; gentamicin, $\chi^2_{12} = 27.4$, corrected $P < 0.05$; streptomycin, $\chi^2_{15} = 33.4$, corrected $P < 0.05$; and trimethoprim, $\chi^2_6 = 52.0$, corrected $P < 0.001$). Despite this, we did not find any evidence of matching between mutants and their selection environments in terms of antibiotic-free growth (sympatric versus allopatric

contrast: $P > 0.05$ for all selection antibiotics). In summary, local abiotic conditions modified the costs of resistance for our genotypes in the absence of antibiotics, but this did not explain the distribution of genotypes across selection environments in our mutant screen.

DISCUSSION

Our findings have important implications for research that aims to exploit collateral sensitivity in novel treatment approaches. For example, among our trimethoprim-resistant mutants, those selected at high temperatures showed the greatest collateral sensitivity to nitrofurantoin. Thus, trimethoprim treatment of poultry (36), with a higher body temperature, could potentially select for mutants that are collaterally sensitive to nitrofurantoin, but this may be less likely in other environments. Studies of collateral sensitivity will therefore be most relevant when they account for environmental variation, for example by focusing on resistant mutants that arise under conditions similar to those during infection, or testing explicitly for variation across abiotic conditions (as done here). This will ensure that collateral effects of mutations specific to the infection environment are not overlooked, and that collaterally sensitive mutants specific to the lab environment are not given undue attention. Note that our study included only chromosomal mutants derived from a single laboratory strain, allowing us to study the mutants in a well-characterized genetic background. Nevertheless, some of the resistance mechanisms we identified are known to be important in natural and clinical populations, such as mutations in genes for efflux pumps (*acr*) (37), global regulators (*marR* and *phoPQ*) (38, 40) and specific antibiotic targets (*ftsI* and *rpsL*) (41–43), suggesting that our findings are relevant beyond laboratory studies. A key question for future work is whether collateral effects of resistance encoded on plasmids (44, 45), which is common in clinics, show sensitivity similar to that under abiotic conditions as we saw here. We speculate that this is likely, because plasmids can carry accessory genes with fitness effects that are strongly affected by the abiotic environment (46, 47). In support, a recent study suggested that plasmid carriage can induce collateral sensitivity in *E. coli* (48).

Some past studies have looked at collateral sensitivity in clinical isolates (10, 49, 50), but these studies each measured collateral sensitivity in a single lab environment. Our results suggest that this may risk overlooking collateral sensitivity interactions that may be important in the infection environment. For example, if we had tested *cpxA* mutants only in a single environment at 37°C, we would have observed only that they mediate cross-resistance between gentamicin and cefuroxime (51, 52). This would miss the collateral sensitivity of these mutants at higher temperature (Fig. 2b), a potentially interesting target for collateral sensitivity in *E. coli* infecting hosts with higher body temperatures, such as poultry (25). More generally, variable collateral effects as we observed here are relevant for understanding the evolution of antibiotic resistance across different conditions or environmental compartments (53) or in infections that start in one location, condition, or host before spreading to others (54, 55). The changing expression of collateral effects with abiotic conditions therefore represents an important variable which should be considered if we are to design robust treatment regimens around collateral sensitivity. Of course, our experiments were still restricted to simplified lab conditions. Our aim here was to demonstrate that even relatively minor (but still relevant to nature) manipulations of the abiotic environment can modify collateral sensitivity interactions. Our finding that such effects are strong suggests other differences between complex within-host or natural environments and *in vitro* screening conditions are likely to modify expression of collateral resistance even further.

It is worth noting that the method we used to generate resistant mutants differs from some other studies on collateral sensitivity (5, 6), where bacteria were exposed to sub-MICs or increasing antibiotic concentrations over multiple growth cycles. In our approach, as in a conventional fluctuation assay screening for antibiotic resistant mutants (56), we grew the ancestral strain in the absence of antibiotics to generate

diversity, before treating with inhibitory concentrations of antibiotics to select for resistance to otherwise inhibitory concentrations. Thus, resistance emerges via selection at a high concentration for preexisting resistant variants (that arose prior to antibiotic exposure), rather than gradual exposure to increasing antibiotic concentrations that progressively increase selection for resistance and decrease population growth of the sensitive ancestral strain (57). We identified many mutations (e.g., in *hem* genes) that have been found in previous studies (5, 10). The method we used also parallels the course of many infections, as an infection is established in the absence of antibiotics and then a dose of antibiotics designed to fully inhibit the infection is used on the diverse population, either wiping it out or strongly selecting for any resistant subpopulation that is present (58, 59). Nevertheless, such single-step screens may select for a subset of all possible pathways to resistance, for example if there are multimutational pathways that emerge only upon gradual exposure (60).

In summary, we found that local abiotic conditions modified collateral sensitivity interactions by two principal mechanisms. First, antibiotic treatment can select for different genetic pathways to resistance depending on the local abiotic environment (Fig. 1). This was the case here for the selection antibiotics cefuroxime and streptomycin, after correcting for multiple testing (under less conservative criteria, this trend is more pervasive across antibiotic treatments). This can in turn alter the average strength of collateral sensitivity to other antibiotics (Fig. 2), as we observed with trimethoprim-resistant mutants, which were variably collaterally sensitive to nitrofurantoin depending on the abiotic environment they were selected in. Second, for individual mutants, expression of collateral sensitivity or cross-resistance can depend strongly on local abiotic conditions. For example, we found that gentamicin-resistant *cpxA* mutants were cross resistant or collaterally sensitive to cefuroxime depending on the assay environment. This is consistent with a more general trend that the phenotypic effects of antibiotic resistance mechanisms are highly sensitive to genotype-by-environment interactions (16–18, 61). Critically, this suggests that for some antibiotic combinations, the effectiveness of the second antibiotic against bacteria that have evolved resistance to the first antibiotic, and consequently selection on resistance to both antibiotics, will depend on the abiotic environment. While collateral sensitivity still holds great promise to prolong the effectiveness of available treatments, we suggest that doing so will be most effective if we account for local abiotic conditions.

MATERIALS AND METHODS

Organisms and growth conditions. We used *Escherichia coli* K-12 MG1655 as the ancestral organism, grown at 37°C in static 100-μl cultures in 96-well microplates unless otherwise stated. The medium used was based on lysogeny broth (LB; Sigma-Aldrich) with additions to create variations in environmental conditions for basal, pH, and bile media. Basal medium (the base condition) is LB buffered at pH 7.0 with 0.1 M sodium hydrogen phosphate (Na_2HPO_4 and NaH_2PO_4). pH medium (acidic pH) is LB buffered at pH 6.5 with 0.1 M sodium hydrogen phosphate. Bile medium is LB with the addition of 0.5 g/liter of bile salts and buffered at pH 7.0 with 0.1 M sodium hydrogen phosphate. The temperature treatment uses the basal medium but is incubated at 42°C. When these conditions were on solid media (i.e., to select for resistant colonies), we instead used LB agar (Sigma-Aldrich), but other temperature and medium additions were the same. For overnight culture prior to assay, we incubated at 37°C in diluted LB (LB-water, 1:2).

Mutant isolation. We screened for mutants resistant to each selection antibiotic in each selection environment by first making 460 cultures of the ancestral *E. coli* strain for each of the 4 selection environments (1,840 cultures total, each inoculated with a small number of cells via dilution from a single frozen stock), incubated for 20 h in the absence of antibiotics. Each entire culture was then transferred to a well of a 24-well plate containing 1 ml of agar corresponding to the same selection environment as the prior liquid culture plus one of five antibiotics at selection concentration (cefuroxime [selection concentration = 6 μg mL^{-1}], chloramphenicol [6 μg mL^{-1}], gentamicin [24 μg mL^{-1}], streptomycin [72 μg mL^{-1}], and trimethoprim [0.5 μg mL^{-1}]). These selection concentrations were approximately equal to MICs for the ancestor. This meant the ancestral strain was effectively inhibited, but mutants with even moderately increased resistance could grow. A higher selection concentration was used for the aminoglycosides (gentamicin, 48 μg mL^{-1}; streptomycin, 144 μg mL^{-1}) in the pH medium because of the reduced efficacy against the ancestral strain in this environment (62). The agar with bacterial culture was incubated for 48 h at 37 or 42°C. This protocol was used to screen 92 independent *E. coli* populations (each plated from a separate overnight culture grown in the absence of antibiotics) for each combination of 4 selection environments and 5 selection antibiotics. After incubation, each agar well was checked for the appearance of resistant colonies (the number of populations that produced at least one

colony is shown in Fig. S6). Up to 6 colonies for each antibiotic-by-environment combination were picked from 6 randomly selected, independent agar wells (populations). These colonies were grown in LB without antibiotics (so as not to further select for resistance) for 3 h before glycerol was added to 25% of the final volume and mutants were frozen at $-80°C$. Mutant isolation in the basal, pH, and temperature environments was done in the same temporal block, and the bile environment in a separate block. These frozen stocks were used to inoculate cultures in LB without antibiotics to extract DNA for sequencing. For a minority of mutants, we were unable to consistently revive the frozen stock for library preparation for sequencing and/or for phenotyping. These were excluded from the relevant assays and analysis (see Table S2 for details).

Genome sequencing and bioinformatics. Genomic DNA from 110 mutants plus the ancestral strain was extracted with the Genomic-tip 20/G kit (catalog no. 10223; Qiagen) according to the manufacturer's instructions. Libraries were produced using the Illumina Nextera XT kit. Sequencing was performed on the Illumina HiSeq 4000 platform with 150-bp paired-end reads at the Functional Genomic Center, Zürich, Switzerland (Fig. 1). Reads were trimmed using Trimmomatic (63) and then analyzed using the breseq pipeline in consensus mode relative to the K-12 MG1655 reference, taking into account mutations present in our ancestral strain (64, 65). For each mutant, we then identified which genes were affected by mutations due to single nucleotide polymorphisms (SNPs) or insertions or deletions in the coding sequence or the promoter region of the gene (identified by breseq or in rare cases by manual curation) (Table S1) relative to the ancestral sequence. Four synonymous SNPs are shown in Fig. 1 but were excluded from our analysis. Several strains did not have mutations identified by breseq in consensus mode and were therefore not used for further analysis. Once we had completed these filtering steps, we gained full genotypic information for 84 strains.

For plotting and analysis, we accounted for differences both among individual mutants, and among genes or gene sets that were mutated in multiple individual mutants. For example, there were multiple mutants with mutations in *ftsI* (Fig. 1). A gene set here is a group of related genes (Table S1), including genes from the same operon (e.g., *phoQP*) or having very closely related functions (e.g., all *rib* genes). In one mutant, we found a large deletion affecting multiple genes, including *hemB*, which was also altered in some other mutants; this mutation was designated as affecting *hemB*. This list of genes and gene sets was used in PERMANOVA (see "Statistics"). Sixteen mutants had multiple mutations affecting multiple genes (Table S1); 11 of these mutants were included in the phenotypic analysis. In such cases, if one of the mutated genes was also mutated in other mutants, we categorized the strain according to this gene (e.g., CFR5Basal, categorized as *marR* because the other mutated gene in this mutant, *asmA*, was not mutated in any other mutant and because *marR* has a known role in resistance); in the other such cases, we categorized each mutant according to mutated genes known to be involved in resistance to the selection antibiotic (e.g., GEN4pH categorized as *nuoG*, because *nuoG* has been associated with resistance previously [5]). The choice of gene used for categorization and labeling did not affect the outcome of our analyses in these latter cases.

Measuring resistance to selection antibiotics and other antibiotics. We selected 75 strains with genotypic information to phenotype (and the ancestor), excluding mutants where very similar genotypes were already represented. Resistance of all mutants and the ancestral strain was quantified using broth dilution. For each antibiotic, we assayed each combination of strain, assay environment, and antibiotic concentration in four biological replicates, each in a separate temporal block. In each block of assays, we used a frozen master plate containing all strains organized in one of three randomized layouts (blocks 1, 2, 3, and 4 used layouts 1, 2, 3, and 1) to inoculate a single preculture plate (LB-water, 1:2). We then incubated the preculture plate for 3 h before using it to inoculate all the overnight plates (for every assay culture, we grew a separate overnight culture). Overnight cultures were then used to inoculate the assay plates using a pin replicator. Each mutant was tested against the relevant selection and paired antibiotics, and the ancestor was tested against all antibiotics, each at 8 concentrations (including zero) in each assay environment. After culturing assay plates for 20 h, we agitated the plates to resuspend bacteria and then measured the biomass of bacteria by optical density at 600 nm (OD_{600}) using a spectrophotometer (Infinite 200 Pro; Tecan Trading AG, Switzerland). Due to the time taken to read 64 plates, incubation and plate reading was staggered and the order was randomized. Some mutants failed to regrow during overnight incubation, resulting in some assay wells not being inoculated. To filter out these false negatives, we excluded OD_{600} scores from assay plates that were <0.03, but only if the OD_{600} in the overnight well (prior to inoculation of the assay well) was also <0.03 (both after subtracting blanks).

Calculation of summary phenotypes from dose-response data. For each mutant strain, we calculated four phenotypes: (i) 90% inhibitory concentration (IC_{90}) of the selection antibiotic, (ii) growth at selection concentration (GASC) for the selection antibiotic, (iii) IC_{90} of the paired antibiotic, and (iv) growth in the absence of antibiotics. These phenotypes were calculated from the dose-response relationship data for the selection and paired antibiotics (for each replicate separately). We fitted a Hill function using nonlinear least-squares analysis in R (66), using the nlsLM function in the minpack.LM package (67): $OD = (A \times k^n)/(k^n + C^n)$, where OD is the measured optical density and C is the antibiotic concentration. A is then the asymptote, k is the inflection point of the curve, and n is the Hill parameter controlling curve steepness. Thus, growth in the absence of antibiotics is equal to A, so for each combination of mutant and assay environment, antibiotic-free growth is the mean of the A parameters across all dose-response curves for this strain and environment. The IC_{90} for the selection and paired antibiotics can be calculated using the following formula, taking the parameters from the relevant fitted curve.

$$IC_{90} = e^{\left[\ln(k) + \frac{\ln(9)}{n}\right]}$$

Finally, GASC is the value of the Hill function when the antibiotic concentration equals the selection concentration.

For some strain-antibiotic-environment combinations, we could not robustly fit a Hill function to some or all replicates, for example if there was very little growth inhibition or if the dose response was strongly stepwise. In these cases, where possible, we calculated phenotypes independently from the fitting of dose response curves (as is often done in other studies [6]). We estimated growth in the absence of antibiotics from the OD measured after growth without antibiotics. We took the IC_{90} as the lowest tested concentration where growth was below 10% of growth in the absence of antibiotics. Finally, we took growth at selection concentration as the OD score at the selection concentration of the antibiotic or the predicted score at the selection concentration, assuming a linear relationship between growth and antibiotic concentration between the two measured concentrations on either side of the selection concentration. We used these fit-independent methods for a minority of cases (4.76% for antibiotic free growth, 2.48% for selection antibiotic IC_{90}, 3.73% for paired-antibiotic IC_{90}, and 4.76% for GASC). In all cases, there was a strong correlation between the fit-dependent and fit-independent measures (Fig. S7).

Statistics. We treated the mutants selected for resistance against different antibiotics as independent data sets, due to the difficulty in comparing resistance across multiple antibiotics. This meant that we had only 5 independent mutants for chloramphenicol, which limited our ability to draw conclusions about this antibiotic. Therefore, we do not discuss the chloramphenicol-resistant mutants in the text, but they are included in the supplemental information for completeness (Fig. S2). In each data set, we took the four phenotypes of interest (see above) as response variables in separate models. In each model, the replicate measures for each phenotype came from independent dose response curves (fitted to data collected in different blocks). Mutants with insufficiently replicated data (<2 replicates in any of the four assay environments) for a given phenotype were excluded from the analysis for that phenotype, meaning that we had between 53 and 57 mutants for each of the 4 phenotypes (Table S2). We transformed IC_{90}s by taking $\log_2(IC_{90})$ relative to the mean of the ancestral strain ($\log_2$ transformed) measured in the same environment. This controlled for any effects of assay environment on antibiotic inhibition of the ancestral strain (Fig. S3) and normalized the data. GASC was square root transformed to fit the assumption of normality but was not relative to the ancestor, as the GASC was not significantly different from zero in the ancestor (as expected, given that we set selection concentrations close to the ancestral MIC). Growth in the absence of antibiotics already fitted the assumption of normality and was not analyzed relative to the ancestor, because ancestral growth did not vary significantly between assay environments ($\chi^2_3 = 5.11$; $P > 0.05$).

For each of the 4 phenotypes across the 4 antibiotic data sets, we fitted two mixed effects models (Table S3). The fixed effects of model A were as follows: phenotype ~ genotype + assay_environment + genotype: assay_environment. Those for model B were as follows: phenotype ~ selection_environment + assay_environment + sympatry. In these models, genotype is based on the gene set mutated (so that mutants with different mutations in the same gene or gene set have the same genotype) (Table S1), and sympatry is a binary vector indicating whether selection environment is the same as assay environment. Model A was used to test whether genotypes varied in their average phenotypes (effect of genotype) and whether that variation depended on the local abiotic conditions (genotype-by-assay-environment interaction). To test the effect of selection environment, we used a separate model (model B), because genotype and selection environment were often confounded. Model B was used to test whether each phenotype varied on average among sets of mutants isolated from different selection environments (effect of selection environment) and for evidence of matching between mutants and their selection environments (higher average phenotypic scores in sympatric compared to allopatric combinations, where sympatry means that selection environment is the same as assay environment, and allopatry means that selection environment is not the same as assay environment; tested by the main effect of sympatry) (34).

In both models, we included a nested random effect of strain (individual mutant ID) on intercept [+(1|Strain) in the lmer function] to account for variation between strains (68). We also included a random effect of block nested within strain on the intercept [+(1|Strain:Block) in the lmer function], to account for variation between measures of the same strain in different blocks. To prevent overfitting, the variance explained by these random effects was tested using a likelihood ratio test (on the maximal model) and nonsignificant terms were dropped, potentially reducing to a fixed-effects model if both random effects were dropped (Table S3). After random effects were tested, we dropped nonsignificant fixed-effect terms to reach minimal models. For model simplification, both fixed-effect and random-effect terms were tested at an α value of 0.05.

Significance of terms in models is reported from minimal models by comparing models with or without the term of interest using an F test for fixed-effects models and a likelihood ratio test (χ^2 statistic) for mixed models. When the main effect of genotype is involved in a significant higher-order interaction (genotype: assay_environment) the main effect cannot be dropped, so significance is instead reported with an F test (on a type III ANOVA), regardless of whether the model contains random effects. For mixed models, the approximate degrees of freedom are calculated using lmerTest (69). Although assay environment is included in both models, we report the significance of the main effect of assay environment from model B, where it does not have higher-order interactions and can always be tested using a likelihood ratio test.

To test whether the genes/gene sets that were mutated varied depending on the selection environment mutants were isolated from, we used a permutational ANOVA on the data for which genes/gene sets were affected by the mutations (Table S2, full genotype). This was performed using the adonis function in the vegan package (70).

For both the genotype and phenotype models, we tested 4 data sets (from four antibiotic combinations) for similar effects in parallel, therefore, when reporting the results of these tests, we give P values corrected for multiple testing using the Holm-Bonferroni method (sequential Bonferroni). These are reported in the text as corrected P values, and values below 0.05 are considered significant.

Data availability. All raw data are available on Dryad (https://doi.org/10.5061/dryad.6m905qg16). Genomic data are relative to the reference genome of *Escherichia coli* K-12 MG1655 and have been uploaded as SNP tables relative to this reference in the Dryad data file.

SUPPLEMENTAL MATERIAL

Supplemental material is available online only.

FIG S1, TIF file, 0.9 MB.
FIG S2, TIF file, 0.3 MB.
FIG S3, TIF file, 0.5 MB.
FIG S4, TIF file, 0.4 MB.
FIG S5, TIF file, 0.1 MB.
FIG S6, TIF file, 0.1 MB.
FIG S7, TIF file, 0.2 MB.
TABLE S1, DOCX file, 0.1 MB.
TABLE S2, DOCX file, 0.04 MB.
TABLE S3, DOCX file, 0.03 MB.

ACKNOWLEDGMENTS

REFERENCES

1. World Health Organization. 2014. Antimicrobial resistance global report on surveillance, p 1–9.
2. Ling LL, Schneider T, Peoples AJ, Spoering AL, Engels I, Conlon BP, Mueller A, Schäberle TF, Hughes DE, Epstein S, Jones M, Lazarides L, Steadman VA, Cohen DR, Felix CR, Fetterman KA, Millett WP, Nitti AG, Zullo AM, Chen C, Lewis K. 2015. A new antibiotic kills pathogens without detectable resistance. Nature 517:455–459. https://doi.org/10.1038/nature14098.
3. Coates AR, Halls G, Hu Y. 2011. Novel classes of antibiotics or more of the same? Br J Pharmacol 163:184–194. https://doi.org/10.1111/j.1476-5381.2011.01250.x.
4. Read AF, Huijben S. 2009. Evolutionary biology and the avoidance of antimicrobial resistance. Evol Appl 2:40–51. https://doi.org/10.1111/j.1752-4571.2008.00066.x.
5. Lázár V, Pal Singh G, Spohn R, Nagy I, Horváth B, Hrtyan M, Busa-Fekete R, Bogos B, Méhi O, Csörgő B, Pósfai G, Fekete G, Szappanos B, Kégl B, Papp B, Pál C. 2013. Bacterial evolution of antibiotic hypersensitivity. Mol Syst Biol 9:700. https://doi.org/10.1038/msb.2013.57.
6. Imamovic L, Sommer MOA. 2013. Use of collateral sensitivity networks to design drug cycling protocols that avoid resistance development. Sci Transl Med 5:204ra132. https://doi.org/10.1126/scitranslmed.3006609.
7. Pál C, Papp B, Lázár V. 2015. Collateral sensitivity of antibiotic-resistant microbes. Trends Microbiol 23:401–407. https://doi.org/10.1016/j.tim.2015.02.009.
8. Baym M, Stone LK, Kishony R. 2016. Multidrug evolutionary strategies to reverse antibiotic resistance. Science 351:aad3292. https://doi.org/10.1126/science.aad3292.
9. Barbosa C, Beardmore R, Schulenburg H, Jansen G. 2018. Antibiotic combination efficacy (ACE) networks for a Pseudomonas aeruginosa model. PLoS Biol 16:e2004356. https://doi.org/10.1371/journal.pbio.2004356.
10. Podnecky NL, Fredheim EGA, Kloos J, Sørum V, Primicerio R, Roberts AP, Rozen DE, Samuelsen Ø, Johnsen PJ. 2018. Conserved collateral antibiotic susceptibility networks in diverse clinical strains of Escherichia coli. Nat Commun 9:3673. https://doi.org/10.1038/s41467-018-06143-y.
11. Nichol D, Rutter J, Bryant C, Hujer AM, Lek S, Adams MD, Jeavons P, Anderson ARA, Bonomo RA, Scott JG. 2019. Antibiotic collateral sensitivity is contingent on the repeatability of evolution. Nat Commun 10:334. https://doi.org/10.1038/s41467-018-08098-6.
12. Barbosa C, Trebosc V, Kemmer C, Rosenstiel P, Beardmore R, Schulenburg H, Jansen G. 2017. Alternative evolutionary paths to bacterial antibiotic resistance cause distinct collateral effects. Mol Biol Evol 34:2229–2244. https://doi.org/10.1093/molbev/msx158.
13. Barbosa C, Römhild R, Rosenstiel P, Schulenburg H. 2019. Evolutionary stability of collateral sensitivity to antibiotics in the model pathogen pseudomonas aeruginosa. Elife 8:1–22. https://doi.org/10.7554/eLife.51481.
14. Maltas J, Wood KB. 2019. Pervasive and diverse collateral sensitivity profiles inform optimal strategies to limit antibiotic resistance. PLoS Biol 17:e3000515. https://doi.org/10.1371/journal.pbio.3000515.
15. Roemhild R, Linkevicius M, Andersson DI. 2020. Molecular mechanisms of collateral sensitivity to the antibiotic nitrofurantoin. PLoS Biol 18:e3000612. https://doi.org/10.1371/journal.pbio.3000612.
16. Hall AR, Angst DC, Schiessl KT, Ackermann M. 2015. Costs of antibiotic resistance—separating trait effects and selective effects. Evol Appl 8:261–272. https://doi.org/10.1111/eva.12187.
17. Paulander W, Maisnier-Patin S, Andersson DI. 2009. The fitness cost of streptomycin resistance depends on rpsL mutation, carbon source and RpoS (σS). Genetics 183:539–546. https://doi.org/10.1534/genetics.109.106104.
18. Petersen A, Aarestrup FM, Olsen JE. 2009. The in vitro fitness cost of antimicrobial resistance in Escherichia coli varies with the growth conditions. FEMS Microbiol Lett 299:53–59. https://doi.org/10.1111/j.1574-6968.2009.01734.x.
19. Trindade S, Sousa A, Gordo I. 2012. Antibiotic resistance and stress in the light of Fisher's model. Evolution 66:3815–3824. https://doi.org/10.1111/j.1558-5646.2012.01722.x.
20. Rosenberg EY, Bertenthal D, Nilles ML, Bertrand KP, Nikaido H. 2003. Bile salts and fatty acids induce the expression of Escherichia coli AcrAB multidrug efflux pump through their interaction with Rob regulatory protein. Mol Microbiol 48:1609–1619. https://doi.org/10.1046/j.1365-2958.2003.03531.x.
21. Lin DL, Tran T, Alam JY, Herron SR, Ramirez MS, Tolmasky ME. 2014. Inhibition of aminoglycoside 6′-N-acetyltransferase type Ib by zinc: reversal of amikacin resistance in Acinetobacter baumannii and Escherichia coli by a zinc ionophore. Antimicrob Agents Chemother 58:4238–4241. https://doi.org/10.1128/AAC.00129-14.
22. Rodríguez-Verdugo A, Gaut BS, Tenaillon O. 2013. Evolution of escherichia coli rifampicin resistance in an antibiotic-free environment during thermal stress. BMC Evol Biol 13:50. https://doi.org/10.1186/1471-2148-13-50.

23. Evans DF, Pye G, Bramley R, Clark AG, Dyson TJ, Hardcastle JD. 1988. Measurement of gastrointestinal pH profiles in normal ambulant human subjects. Gut 29:1035–1041. https://doi.org/10.1136/gut.29.8.1035.

24. Wagner C, Sauermann R, Joukhadar C. 2006. Principles of antibiotic penetration into abscess fluid. Pharmacology 78:1–10. https://doi.org/10.1159/000094668.

25. Troxell B, Petri N, Daron C, Pereira R, Mendoza M, Hassan HM, Koci MD. 2015. Poultry body temperature contributes to invasion control through reduced expression of Salmonella pathogenicity island 1 genes in Salmonella enterica serovars typhimurium and enteritidis. Appl Environ Microbiol 81:8192–8201. https://doi.org/10.1128/AEM.02622-15.

26. Gunn JS. 2000. Mechanisms of bacterial resistance and response to bile. Microbes Infect 2:907–913. https://doi.org/10.1016/s1286-4579(00)00392-0.

27. Muir ME, Hanwell DR, Wallace BJ. 1981. Characterization of a respiratory mutant of Escherichia coli with reduced uptake of aminoglycoside antibiotics. Biochim Biophys Acta 638:234–241. https://doi.org/10.1016/0005-2728(81)90232-2.

28. Mahoney TF, Silhavy TJ. 2013. The Cpx stress response confers resistance to some, but not all, bactericidal antibiotics. J Bacteriol 195:1869–1874. https://doi.org/10.1128/JB.02197-12.

29. Raivio TL, Silhavy TJ. 1997. Transduction of envelope stress in Escherichia coli by the Cpx two-component system. J Bacteriol 179:7724–7733. https://doi.org/10.1128/jb.179.24.7724-7733.1997.

30. McEwen J, Silverman PM. 1982. Mutations in genes cpxA and cpxB alter the protein composition of Escherichia coli inner and outer membranes. J Bacteriol 151:1553–1559. https://doi.org/10.1128/jb.151.3.1553-1559.1982.

31. Pogliano J, Dong JM, De Wulf P, Furlong D, Boyd D, Losick R, Pogliano K, Lin ECC. 1998. Aberrant cell division and random FtsZ ring positioning in Escherichia coli cpxA* mutants. J Bacteriol 180:3486–3490. https://doi.org/10.1128/JB.180.13.3486-3490.1998.

32. Delhaye A, Collet JF, Laloux G. 2016. Fine-tuning of the Cpx envelope stress response is required for cell wall homeostasis in Escherichia coli. mBio 7:e00047-16. https://doi.org/10.1128/mBio.00047-16.

33. Kawecki TJ, Ebert D. 2004. Conceptual issues in local adaptation. Ecol Lett 7:1225–1241. https://doi.org/10.1111/j.1461-0248.2004.00684.x.

34. Blanquart F, Kaltz O, Nuismer SL, Gandon S. 2013. A practical guide to measuring local adaptation. Ecol Lett 16:1195–1205. https://doi.org/10.1111/ele.12150.

35. Andersson DI, Hughes D. 2010. Antibiotic resistance and its cost: is it possible to reverse resistance? Nat Rev Microbiol 8:260–271. https://doi.org/10.1038/nrmicro2319.

36. Economou V, Gousia P. 2015. Agriculture and food animals as a source of antimicrobial-resistant bacteria. Infect Drug Resist 8:49–61. https://doi.org/10.2147/IDR.S55778.

37. Webber MA, Piddock LJV. 2001. Absence of mutations in marRAB or soxRS in acrB-overexpressing fluoroquinolone-resistant clinical and veterinary isolates of Escherichia coli. Antimicrob Agents Chemother 45:1550–1552. https://doi.org/10.1128/AAC.45.5.1550-1552.2001.

38. Luo Q, Yu W, Zhou K, Guo L, Shen P, Lu H, Huang C, Xu H, Xu S, Xiao Y, Li L. 2017. Molecular epidemiology and colistin resistant mechanism of mcr-positive and mcr-negative clinical isolated Escherichia coli. Front Microbiol 8:2262. https://doi.org/10.3389/fmicb.2017.02262.

39. Reference deleted.

40. Atac N, Kurt-Azap O, Dolapci I, Yesilkaya A, Ergonul O, Gonen M, Can F. 2018. The role of AcrAB–TolC efflux pumps on quinolone resistance of E. coli ST131. Curr Microbiol 75:1661–1666. https://doi.org/10.1007/s00284-018-1577-y.

41. Patiño-Navarrete R, Rosinski-Chupin I, Cabanel N, Gauthier L, Takissian J, Madec JY, Hamze M, Bonnin RA, Naas T, Glaser P. 2020. Stepwise evolution and convergent recombination underlie the global dissemination of carbapenemase-producing Escherichia coli. Genome Med 12:10–18. https://doi.org/10.1186/s13073-019-0699-6.

42. Pelchovich G, Schreiber R, Zhuravlev A, Gophna U. 2013. The contribution of common rpsL mutations in Escherichia coli to sensitivity to ribosome targeting antibiotics. Int J Med Microbiol 303:558–562. https://doi.org/10.1016/j.ijmm.2013.07.006.

43. Phelan J, Coll F, McNerney R, Ascher DB, Pires DEV, Furnham N, Coeck N, Hill-Cawthorne GA, Nair MB, Mallard K, Ramsay A, Campino S, Hibberd ML, Pain A, Rigouts L, Clark TG. 2016. Mycobacterium tuberculosis whole genome sequencing and protein structure modelling provides insights into anti-tuberculosis drug resistance. BMC Med 14:1–13. https://doi.org/10.1186/s12916-016-0575-9.

44. Fröhlich C, Sørum V, Thomassen AM, Johnsen PJ, Leiros H-KS, Samuelsen Ø. 2019. OXA-48-mediated ceftazidime-avibactam resistance is associated with evolutionary trade-offs. mSphere 4:e00024-19. https://doi.org/10.1128/mSphere.00024-19.

45. Rosenkilde CEH, Munck C, Porse A, Linkevicius M, Andersson DI, Sommer MOA. 2019. Collateral sensitivity constrains resistance evolution of the CTX-M-15 β-lactamase. Nat Commun 10:618. https://doi.org/10.1038/s41467-019-08529-y.

46. San Millan A, Toll-Riera M, Qi Q, Betts A, Hopkinson RJ, McCullagh J, MacLean RC. 2018. Integrative analysis of fitness and metabolic effects of plasmids in Pseudomonas aeruginosa PAO1. ISME J 12:3014–3024. https://doi.org/10.1038/s41396-018-0224-8.

47. Johnson TJ, Nolan LK. 2009. Pathogenomics of the virulence plasmids of Escherichia coli. Microbiol Mol Biol Rev 73:750–774. https://doi.org/10.1128/MMBR.00015-09.

48. Herencias C, Rodríguez-Beltrán J, León-Sampedro R, Alonso-del Valle A, Palkovičová J, Cantón R, Millán ÁS. 2020. Collateral sensitivity associated with antibiotic resistance plasmids. Elife 10:e65130. https://doi.org/10.7554/eLife.65130.

49. Imamovic L, Ellabaan MMH, Dantas Machado AM, Citterio L, Wulff T, Molin S, Krogh Johansen H, Sommer MOA. 2018. Drug-driven phenotypic convergence supports rational treatment strategies of chronic infections. Cell 172:121–134.E14. https://doi.org/10.1016/j.cell.2017.12.012.

50. Jansen G, Mahrt N, Tueffers L, Barbosa C, Harjes M, Adolph G, Friedrichs A, Krenz-Weinreich A, Rosenstiel P, Schulenburg H. 2016. Association between clinical antibiotic resistance and susceptibility of Pseudomonas in the cystic fibrosis lung. Evol Med Public Health 2016:182–194. https://doi.org/10.1093/emph/eow016.

51. Lázár V, Nagy I, Spohn R, Csörgő B, Györkei Á, Nyerges Á, Horváth B, Vörös A, Busa-Fekete R, Hrtyan M, Bogos B, Méhi O, Fekete G, Szappanos B, Kégl B, Papp B, Pál C. 2014. Genome-wide analysis captures the determinants of the antibiotic cross-resistance interaction network. Nat Commun 5:4352. https://doi.org/10.1038/ncomms5352.

52. Oz T, Guvenek A, Yildiz S, Karaboga E, Tamer YT, Mumcuyan N, Ozan VB, Senturk GH, Cokol M, Yeh P, Toprak E. 2014. Strength of selection pressure is an important parameter contributing to the complexity of antibiotic resistance evolution. Mol Biol Evol 31:2387–2401. https://doi.org/10.1093/molbev/msu191.

53. Berendonk TU, Manaia CM, Merlin C, Fatta-Kassinos D, Cytryn E, Walsh F, Bürgmann H, Sørum H, Norström M, Pons M-N, Kreuzinger N, Huovinen P, Stefani S, Schwartz T, Kisand V, Baquero F, Martinez JL. 2015. Tackling antibiotic resistance: the environmental framework. Nat Rev Microbiol 13:310–317. https://doi.org/10.1038/nrmicro3439.

54. León-Sampedro R, DelaFuente J, Díaz-Agero C, Crellen T, Musicha P, Rodríguez-Beltrán J, de la Vega C, Hernández-García M, López-Fresneña N, Ruiz-Garbajosa P, Cantón R, Cooper BS, San Millán Á, Group R-GWS. 2021. Pervasive transmission of a carbapenem resistance plasmid in the gut microbiota of hospitalized patients. Nat Microbiol 6:606–616. https://doi.org/10.1038/s41564-021-00879-y.

55. Gygli SM, Loiseau C, Jugheli L, Adamia N, Trauner A, Reinhard M, Ross A, Borrell S, Aspindzelashvili R, Maghradze N, Reither K, Beisel C, Tukvadze N, Avaliani Z, Gagneux S. 2021. Prisons as ecological drivers of fitness-compensated multidrug-resistant Mycobacterium tuberculosis. Nat Med 27:1171–1177. https://doi.org/10.1038/s41591-021-01358-x.

56. Pope CF, O'Sullivan DM, McHugh TD, Gillespie SH. 2008. A practical guide to measuring mutation rates in antibiotic resistance. Antimicrob Agents Chemother 52:1209–1214. https://doi.org/10.1128/AAC.01152-07.

57. Kouyos RD, Metcalf CJE, Birger R, Klein EY, Zur Wiesch PA, Ankomah P, Arinaminpathy N, Bogich TL, Bonhoeffer S, Brower C, Chi-Johnston G, Cohen T, Day T, Greenhouse B, Huijben S, Metlay J, Mideo N, Pollitt LC, Read AF, Smith DL, Standley C, Wale N, Grenfell B. 2014. The path of least resistance: aggressive or moderate treatment? Proc R Soc Lond B Biol Sci 281:20140566. https://doi.org/10.1098/rspb.2014.0566.

58. European Centre for Disease Prevention and Control. 2000. Antimicrobial resistance in the EU/EEA (EARS-Net)—annual epidemiological report for 2019. European Centre for Disease Prevention and Control, Stockholm, Sweden.

59. Bell G, MacLean C. 2018. The search for 'evolution-proof' antibiotics. Trends Microbiol 26:471–483. https://doi.org/10.1016/j.tim.2017.11.005.

60. Lindsey HA, Gallie J, Taylor S, Kerr B. 2013. Evolutionary rescue from extinction is contingent on a lower rate of environmental change. Nature 494:463–467. https://doi.org/10.1038/nature11879.

61. Santos-Lopez A, Marshall CW, Scribner MR, Snyder DJ, Cooper VS. 2019. Evolutionary pathways to antibiotic resistance are dependent upon environmental structure and bacterial lifestyle. Elife 8:8–10. https://doi.org/10.7554/eLife.47612.

62. Damper PD, Epstein W. 1981. Role of the membrane potential in bacterial resistance to aminoglycoside antibiotics. Antimicrob Agents Chemother 20:803–808. https://doi.org/10.1128/AAC.20.6.803.

63. Bolger AM, Lohse M, Usadel B. 2014. Trimmomatic: a flexible trimmer for Illumina sequence data. Bioinformatics 30:2114–2120. https://doi.org/10.1093/bioinformatics/btu170.

64. Barrick JE, Colburn G, Deatherage DE, Traverse CC, Strand MD, Borges JJ, Knoester DB, Reba A, Meyer AG. 2014. Identifying structural variation in haploid microbial genomes from short-read resequencing data using breseq. BMC Genomics 15:1039. https://doi.org/10.1186/1471-2164-15-1039.

65. Deatherage DE, Barrick JE. 2014. Identification of mutations in laboratory-evolved microbes from next-generation sequencing data using breseq. Methods Mol Biol 1151:165–188. https://doi.org/10.1007/978-1-4939-0554-6_12.

66. Regoes RR, Wiuff C, Zappala RM, Garner KN, Baquero F, Levin BR. 2004. Pharmacodynamic functions: a multiparameter approach to the design of antibiotic treatment regimens. Antimicrob Agents Chemother 48:3670–3676. https://doi.org/10.1128/AAC.48.10.3670-3676.2004.

67. Elzhov TV, Mullen KM, Spiess A-N, Bolker B. 2016. minpack.lm: R interface to the Levenberg-Marquardt nonlinear least-squares algorithm found in MINPACK, plus support for bounds.

68. Bates D, Mächler M, Bolker BM, Walker SC. 2015. Fitting linear mixed-effects models using lme4 67.

69. Kuznetsova A, Brockhoff PB, Christensen RHB. 2017. lmerTest package: tests in linear mixed effects models. J Stat Softw 82:1–26.

70. Oksanen J, Blanchet FG, Friendly M, Kindt R, Legendre P, McGlinn D, Minchin PR, O'Hara RB, Simpson GL, Solymos P, Stevens MHH, Szoecs E, Wagner H. 2019. vegan: Community Ecology Package.